Evidence of Supercritical Behavior in Liquid Single Crystal Elastomers

A. Lebar,[1] Z. Kutnjak,[1] S. Žumer,[2,1] H. Finkelmann,[3] A. Sánchez-Ferrer,[3] and B. Zalar[1]

[1]*J. Stefan Institute, Jamova 39, SI-1000 Ljubljana, Slovenia*

[2]*Department of Physics, University of Ljubljana, Jadranska 19, SI-1000 Ljubljana, Slovenia*

[3]*Institut für Makromolekulare Chemie, Universität Freiburg, D-79104 Freiburg, Germany*

(Received 30 November 2004; published 16 May 2005)

Temperature profiles of the first and the second moment of the nematic order parameter distribution function, as determined from the deuteron nuclear magnetic resonance line shapes, as well as heat capacity response, provide support for the supercritical scenario of the nematic-paranematic phase transition in liquid single crystal elastomers. The relative strength of the locked-in internal mechanical field with respect to the critical field can be decreased by swelling the elastomer samples with low molecular mass nematogen. By increasing the concentration of the dopant, critical and below-critical behavior is promoted.

DOI: 10.1103/PhysRevLett.94.197801 PACS numbers: 64.70.Md, 76.60.−k, 82.70.−y

One of the major open problems in the physics of liquid single crystal elastomers (LSCE) is the nature of the isotropic-nematic phase transition, particularly in view of the question of whether the elasticity in these materials is of the soft, semisoft, or non-soft-type [1]. It was demonstrated [2,3] that the shape of the stress-strain diagram is strongly related to the orientational order of the nematic director field. The degree of this order crucially depends on the crosslinking history of the sample [4]. The debate about the applicability of the concept of soft elasticity to LSCEs has been recently reopened by the measurements of dynamical shear modulus [5]. Conventional nematogenic liquid crystals exhibit a first-order phase transition, easily identifiable by a discontinuous jump of the nematic order parameter (OP) $S(T)$ at the clearing temperature T_{NI}, observed in birefringence measurements [6] or deuteron nuclear magnetic resonance (DNMR) [7] and by a discontinuous jump of the enthalpy observed in calorimetric experiments [8]. In LSCEs, on the contrary, the onset of the nematic order is continuous [7], with a transition from the paranematic (PN) phase with small S to the nematic (N) phase with large S that takes place within a relatively narrow temperature interval (typically a few K). In view of the application potential of these materials for actuator and biomimetic devices (like artificial muscles) [9], the understanding of the physical mechanisms leading to the smearing out of the $S(T)$ profile could contribute to the optimization of the temperature response of mechanical strain, $e(T) \propto S(T)$, for various applications.

There exist two radically different descriptions of the N-PN phase transition in LSCEs. The first one considers them as inherently heterogeneous materials [10], composed of domains, each with a well-defined set of Landau–de Gennes (LdG) free energy expansion coefficients. The average OP temperature profile of the system, $[S]_{\mathrm{av}}(T)$, is then calculated as a superposition of profiles $S(T)$ arising from the individual microdomains. Alternatively, the behavior of $S(T)$ in LSCEs can be attributed to the supercritical character of the N-PN transition [11]. It is a well-known fact that a linear coupling of the nematic OP with a conjugate internal or external field g, accounted for by the free energy term $-gS$, can drive the transition to a supercritical regime, characterized by zero latent heat and continuous $S(T)$ profile. This occurs whenever g exceeds the critical value g_c. In LSCEs, g is the mechanical stress field that consists of the internal, monodomain-state maintaining field g_{int}, imprinted into the system during the two-step ''Finkelmann crosslinking procedure'' [12] and the external field g_{ext}, applied by straining the sample.

The ''heterogeneous'' and ''supercritical'' scenaria, described above, both provide for qualitatively satisfactory description of the OP temperature profile in LSCEs. In order to distinguish between the two scenaria, Selinger *et al.* exploited the fact that, in the N-PN transition region, the two models predict slightly mismatching $S(T)$ curves [10]. They found the internal field to be far below the critical value ($g_{\mathrm{int}}/g_c \sim 0.2$–$0.5$), a result quite unexpected.

In this Letter, we present a novel experimental method which allows for a clear-cut discrimination between the two proposed N-PN transition scenaria. We show that LSCEs, prepared by the ''Finkelmann procedure,'' are supercritical systems with relatively low heterogeneity. We also demonstrate that, when doped with an increasing amount of conventional nematogen, they can be driven towards the critical regime. The method is based on the analysis of the temperature profiles of the first and second moments of DNMR spectra of deuterated mesogenic molecules. Our approach has two advantages over the previous study [10]. First, the primary OP $S(T)$ is analyzed rather than the secondary OP $e(T)$, and, second, we overcome the problems with low resolution, arising from the fact that the experimental error of the $e(T)$ points is of the same order of magnitude as the difference between the theoretical $e(T)$ points of the heterogeneous and supercritical scenaria. The results of the DNMR method are supported by the ac and relaxation calorimetric data.

Side-chain LSCE materials based on poly-[oxy(methylsilylene)] were synthesized as described in

Ref. [12]. Accordingly, the second crosslinking step was carried out in the nematic state. Four samples were prepared. During the second crosslinking step, the first three were loaded with a standard stress of about 10 mN mm^{-2}. The fourth one was allowed longer time for crosslinking in the first step and was submitted to a higher stress of about 50 mN mm^{-2} in the second step. In this way, a stronger internal field $g_{\rm int}$ was expected to be locked in the system. DNMR sensitivity was provided by subsequent doping with octylcyanobiphenyl, deuterated at the two alpha positions in the hydrocarbon chain (8CB-αd_2). This was achieved by initially swelling the elastomer in the controlled molarity solution of 8CB in cyclohexane, to which toluene was subsequently added in small steps to progressively and nondestructively swell the sample to about 400% of its initial volume. After being soaked for a few hours at $T = 330$ K, samples were deswollen to their initial volume by drying in the vacuum rotavapor at the same temperature. Ready for measurements, they contained $x = 0.28$, 0.08, 0.03*, and 0.006 weight concentration of 8CB, respectively, and were marked accordingly as LSCE-x. The star denotes a higher internal field. Since 8CB-αd_2 is itself a nematogen with a first-order N-I transition at $T_{\rm NI}^{(8{\rm CB})} = 315$ K, the increase of x should, apart from the drop in the N-PN transition temperature, $T_{\text{N-PN}}(x \neq 0) < T_{\text{N-PN}}(x = 0) \sim 356$ K, result in the change of the character of the transition from the supposedly supercritical regime for $x = 0$ towards the critical or below-critical regime for high enough x.

DNMR spectra were taken at the deuteron Larmor frequency $\nu_L = 58.4$ MHz on cooling the samples from $T \sim 380$ K. Samples were oriented in the external magnetic field $\mathbf{B}_0$ so that their uniaxiality axis $\mathbf{c}$ pointed along the field. Representative temperature dependencies are shown in Fig. 1. The misalignment of domains in real samples is measured by $\cos\theta = \mathbf{n} \cdot \mathbf{c}$, where $\mathbf{n}$ denotes the local director and $\mathbf{c}$ corresponds to the average director $\overline{\mathbf{n}}$. DNMR spectrum $f(\nu)$ of an 8CB-αd_2 molecule confined to a N or PN domain with OP S and director orientation θ is a doublet of sharp resonance peaks that can be written in terms of Dirac δ-functions:

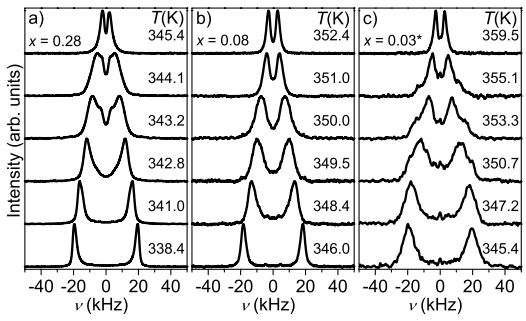

FIG. 1. Temperature dependences of the DNMR line shapes at the orientation $\mathbf{c} \parallel \mathbf{B}_0$: (a) LSCE-0.28, (b) LSCE-0.08, (c) LSCE-0.03*.

$$f(\nu) = \tfrac{1}{2}\{\delta[\nu + \tfrac{3}{4}\nu_q S P_2(\cos\theta)] + \delta[\nu - \tfrac{3}{4}\nu_q S P_2(\cos\theta)]\}. \quad (1)$$

Here $\nu_q \sim 60$ kHz represents the effective quadrupole coupling constant of the αd_2 deuterons and P_2 is the second Legendre polynomial. The frequency offset ν is measured with respect to the Larmor frequency ν_L. The distribution function of $\mathbf{n}$ must possess cylindrical symmetry about $\mathbf{c}$, so that it can be expanded in terms of Legendre polynomials as $w_{\mathbf{n}}(\cos\theta) = \frac{1}{4\pi}\sum_{l=0}^{\infty}(2l+1)S_l P_l(\cos\theta)$. Coefficients S_l are the director OPs. In a nematic state $S_l = 0$ for odd l. Different domains can also exhibit different orientational order S. This disorder can be accounted for by a distribution function $w_S(S)$. With an assumption that the above two distributions are uncorrelated, $w(\cos\theta, S) = w_{\mathbf{n}}(\cos\theta) w_S(S)$, the cumulative DNMR spectrum $F(\nu)$, calculated as the average of $f(\nu; \cos\theta, S)$ [Eq. (1)] over $w(\cos\theta, S)$, can be expressed as a superposition of two mirrored components, $F(\nu) = [\tilde{F}(\nu) + \tilde{F}(-\nu)]/2$, with

$$\tilde{F}(\nu) = \frac{2}{9\nu_q}\sum_{l=0}^{\infty}(2l+1)S_l\int_{-(1/2)}^{1} w_S(S)\tilde{f}_l(\nu, S)dS; \quad (2a)$$

$$\tilde{f}_l(\nu, S) = \begin{cases} \frac{P_l[\sqrt{3}^{-1}(1+\frac{8\nu}{3\nu_q S})^{1/2}]}{S\sqrt{3}^{-1}(1+\frac{8\nu}{3\nu_q S})^{1/2}}; & -\frac{3}{8}\nu_q < \frac{\nu}{S} \leq \frac{3}{4}\nu_q, \\ 0; & \text{otherwise.} \end{cases} \quad (2b)$$

The shape of the DNMR spectrum depends on $w_S(S)$ as well as on the director OPs $\{S_l\}$. Moreover, dynamical processes like fluctuations of the nematic or director OP or (restricted) molecular diffusion can substantially alter the spectrum. This problem is particularly acute with guest 8CB molecules which are free to diffuse over the LSCE network. In order to determine the ''static'' parameters of the LSCE network, $w_S(S)$ and $\{S_l\}$, without having to consider dynamical aspects, one must probe spectral parameters which are independent of the motion of deuteron spins. The first moment $M_1 = \int_{-\infty}^{\infty}\nu\tilde{F}(\nu)d\nu$ and the second moment $M_2 = \int_{-\infty}^{\infty}[\nu - M_1]^2\tilde{F}(\nu)d\nu$ of the DNMR spectrum indeed satisfy this requirement and are easily integrable from $\tilde{F}(\nu)$:

$$M_1 = \frac{3}{4}\nu_q[S]_{\rm av}S_2, \quad (3a)$$

$$M_2 = \frac{9}{16}\nu_q^2[S^2]_{\rm av}\left(\frac{18}{35}S_4 + \frac{2}{7}S_2 + \frac{1}{5}\right) - M_1^2. \quad (3b)$$

$[\ldots]_{\rm av}$ denotes the average over $w_S(S)$. In the case of ideal domain alignment, i.e., for $S_2 = S_4 = 1$, the spectral second moment directly probes the disorder in S, as $M_2 = 9/16\nu_q^2([S^2]_{\rm av} - [S]_{\rm av}^2)$. If in addition the nematic order is homogeneous, like in the supercritical scenario, M_2 vanishes, since in such a case $[S^2]_{\rm av} = [S]_{\rm av}^2$. A problem encountered in practice is that M_1 and M_2 are calculated from $\tilde{F}(\nu)$ and not from $F(\nu)$. One must therefore first decompose the spectrum $F(\nu)$ into its mirrored components $\tilde{F}(\nu)$ and $\tilde{F}(-\nu)$. This is possible if the two components are well separated, a condition well satisfied at the orientation $\mathbf{c} \parallel \mathbf{B}_0$ for which the experimental temperature de-

pendencies of M_1 and M_2 are shown in Fig. 2. Because of an extremely small content of 8CB-αd_2, DNMR spectra of the LSCE-0.006 specimen were too noisy to extract reliable data.

Let us now theoretically model M_1 and M_2 by assuming that the director disorder is quenched, i.e., that the distribution $w_{\mathbf{n}}(\cos\theta)$ and consequently $\{S_l\}$ are all T-independent. We also approximate the director distribution function by a "spherical Gaussian" $w_{\mathbf{n}}(\cos\theta) \propto \exp[(\cos^2\theta - 1)/(2\cos^2\theta \tan^2\sigma_\theta)]$, so that all director OPs can be expressed in terms of σ_θ which describes the angular dispersion of director orientations about $\mathbf{c}$. Furthermore, the "heterogeneity" scenario is modeled by a Gaussian distribution of nominal transition temperatures T^* with mean value $\overline{T}^*$ and dispersion σ_{T^*} [10]:

$$w_S(S;T) \propto \int e^{-[(T^*-\overline{T}^*)^2/(2\sigma_{T^*}^2)]}\delta[S - S_{\mathrm{LdG}}(T)]dT^*. \quad (4)$$

Here the nematic order parameter $S_{\mathrm{LdG}}(T)$ is obtained from the minimization of the LdG free energy [11]

$$F(S,T) = F_0 + \frac{a}{2}(T - T^*)S^2 + \frac{b}{3}S^3 + \frac{c}{4}S^4 - gS. \quad (5)$$

We disregarded the fact that microdomains are mechanically coupled, i.e., that they impose additional local mechanical fields upon each other due to heterogeneity-related random mechanical microdeformations. A strict treatment of such a situation would inevitably involve: (i) dealing with a microscopic model with randomly coupled degrees of freedom [13] and (ii) dropping assumptions of uncorrelated distributions $w_{\mathbf{n}}(\cos\theta)$ and $w_S(S)$ and of T-independent director OPs. This task is, however, far beyond the scope of this Letter. Equation (5) implies that $S_{\mathrm{LdG}}(T)$ is discontinuous at the clearing temperature $T_{\mathrm{NI}} = T^* + 2b^2/(9ac) - 3cg/(ab)$ for internal field values g that are below the critical value $g_c = -b^3/(27c^2)$, whereas it becomes a continuous function of T for $g \geq g_c$. Averages $[S]_{\mathrm{av}}$ and $[S^2]_{\mathrm{av}}$, calculated from Eq. (4), are inserted into Eqs. (3) to express the theoretical spectral moments M_1 and M_2 in terms of T and parameters $\overline{T}^*$, σ_{T^*}, a, b, c, g, and σ_θ. In this way, the three basic structural characteristics of LSCEs are encompassed: the heterogeneity, quantified by σ_{T^*}, the internal mechanical field g, and the misalignment of domains, quantified by σ_θ. Simultaneous fits (with a single set of parameters for both M_1 and M_2) to the experimental $M_1(T)$ and $M_2(T)$ data are shown in Figs. 2(a) and 2(b). The respective relevant best fit parameters (Table I) carry small errors despite their relatively large number. As anticipated, the nominal clearing temperature $\overline{T}_{\mathrm{NI}} = \overline{T}^* + 2b^2/(9ac) - 3cg/(ab)$ increases with decreasing x and approaches its limiting value $\overline{T}_{\mathrm{NI}}(x = 0) \sim 356$ K. As evident from Fig. 2, $\overline{T}_{\mathrm{NI}}$ coincides with the temperature of the $M_2(T)$ maximum in all samples. This provides for a direct experimental determination of $\overline{T}_{\mathrm{NI}}$. The relatively high values of S_2 confirm that samples retain their monodomain state even after being treated with low molecular mass mesogen.

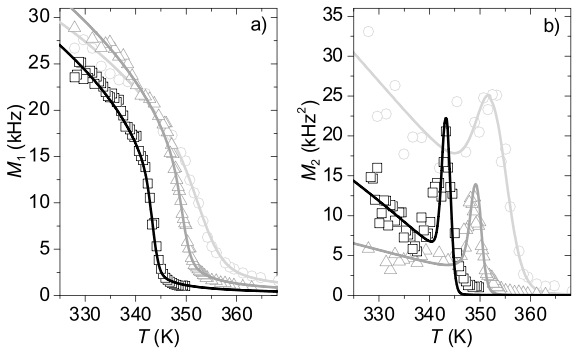

FIG. 2. Temperature dependences of (a) the first and (b) the second moments of DNMR line shapes for LSCE-0.28 (squares), LSCE-0.08 (triangles), and LSCE-0.03* (circles). Theoretical fits are shown as solid lines of matching gray levels (see Table I for fit parameters).

We stress that it is the second moment of the spectrum, M_2, and not the first moment, M_1, which distinguishes between the prevalently heterogeneous (wide σ_{T^*}, $g < g_c$) regime and the prevalently supercritical (narrow σ_{T^*}, $g \geq g_c$) regime. This fact is most convincingly demonstrated by fitting the M_1 experimental data (only the LSCE-0.08 sample is considered) to the "ideal homogeneity" scenario ($\sigma_{T^*} = 0$, $g \neq 0$), which yields $g/g_c = 2 \pm 0.2$ and to the scenario with critical internal field ($\sigma_{T^*} \neq 0$, $g = g_c$), which yields $\sigma_{T^*} = 1.8 \pm 0.2$ K. The two corresponding $M_1(T)$ theoretical curves are practically indistinguishable from the $\sigma_{T^*} \neq 0$, $g \neq 0$ best fit $M_1(T)$ curves [Fig. 3(a)]. On the other hand, the two respective $M_2(T)$ curves, calculated with same parameters as the $M_1(T)$ curves, depart substantially from the $\sigma_{T^*} \neq 0$, $g \neq 0$ best fit $M_2(T)$ curve [Fig. 3(b)]. A general observation not in favor of the heterogeneity scenario [10] is that modeling of experimental $M_1(T)$ with $\sigma_{T^*} \neq 0$ and $g < g_c$ yields greatly exaggerated maxima in $M_2(T)$ with respect to the experimental data.

The supercritical nature of the investigated samples is clearly evidenced from Table I. Specifically, the increase of g/g_c from the value $\sim$1.5 in LSCE-0.08 to $\sim$2.5 in LSCE-0.03* confirms the presumption on stronger internal field in the second sample. Even in the LSCE-0.28 sample, swollen with a relatively high concentration of 8CB that promotes below-critical behavior, g is only slightly below critical ($g/g_c \sim 0.95$). Nevertheless, in all samples a certain degree of heterogeneity coexists with internal fields; we find values of σ_{T^*} (Table I) that are similar to those

TABLE I. Parameters of best theoretical fits to the experimental DNMR line shape moments M_1 and M_2 in LSCEs.

x	g/g_c	σ_{T^*} (K)	$\overline{T}_{\mathrm{NI}}$ (K)	σ_θ(°)	$S_2(\sigma_\theta)$
0.28	0.95 ± 0.1	1.0 ± 0.2	343.4 ± 0.2	14 ± 1	0.86 ± 0.02
0.08	1.5 ± 0.1	1.0 ± 0.2	349.6 ± 0.2	10 ± 1	0.92 ± 0.01
0.03*	2.4 ± 0.25	3.0 ± 0.3	353.9 ± 0.2	17 ± 2	0.82 ± 0.03

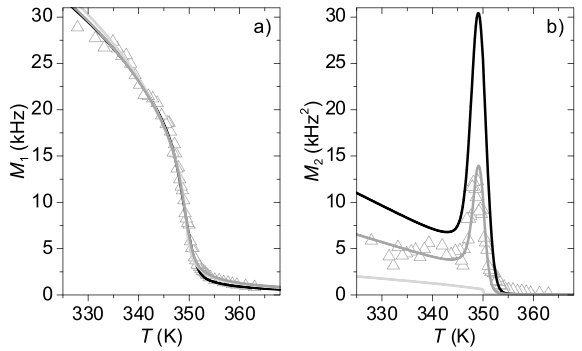

FIG. 3. (a) Best $\sigma_{T^*} = 0$ fit (light gray solid line) and best $g = g_c$ fit (black solid line) to the $M_1(T)$ data (triangles) for LSCE-0.08. Parameters are given in the text. Also added is the overall best fit from Fig. 2(a) (dark gray solid line). (b) $M_2(T)$ theoretical curves, calculated with parameters used to generate the $M_1(T)$ curves.

determined by Selinger *et al.* [10]. Let us note that relation (4) can be generalized to an arbitrary distribution of LdG parameters T^*, a, b, c, and g. Specifically, Gaussian distributions in T^* and g, individually or in both parameters, lead to a Gaussian distribution in T_{NI}, due to a linear relationship among T_{NI}, T^*, and g. However, the $w_S(T)$ profile corresponding to the disorder in T^* differs from the one corresponding to the disorder in g. This is so since the changes in T^* merely result in a shift of T_{NI} while the shape of $S_{\mathrm{LdG}}(T)$ is preserved, whereas changes in g also alter the temperature profile of S_{LdG} [10]. We find that high temperature tails of $M_2(T)$ can be reproduced more perfectly by also considering distributed internal fields.

The above DNMR results are consistently supported by the heat capacity data obtained in the ac and relaxation modes on the same samples. The relaxation mode has much better sensitivity to latent heat L than the ac mode [14]. The comparison between the ac and relaxation heat capacity data (Fig. 4) allows for a quantitative estimation of the latent heat share in the total enthalpy change $\Delta H = \int C_p dT$ due to the first-order phase conversion. The matching ac and relaxation data in LSCE-0.006 indicate zero latent heat, whereas the mismatch in LSCE-0.28 reveals nonzero

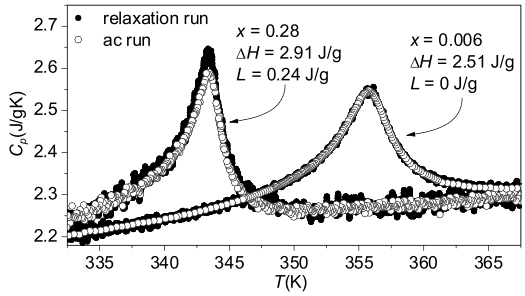

FIG. 4. Heat capacity variations obtained from the relaxation run (solid circles) and ac run (open circles) in LSCE-0.006 and LSCE-0.28. The difference between the relaxation and ac data in LSCE-0.28 indicates nonzero latent heat.

latent heat $L = 0.24\,\mathrm{J/g}$, evidently related to slightly below-critical behavior as indeed observed in DNMR. The width of the anomaly in LSCE-0.28 agrees rather well with σ_{T^*} (see Table I). We note that the heat capacity anomaly becomes significantly broader in LSCE-0.006, in accordance with the proposed supercritical character of the N-PN phase conversion in the $x \rightarrow 0$ limit (virgin LSCEs).

In conclusion, we show for the first time that temperature dependencies of the first and the second moment of the DNMR line shapes in LSCE elastomers clearly reflect the supercritical nature of the N-PN transition. Moreover, we demonstrate that the relative strength (with respect to g_c) of the frozen-in internal fields can be set not only by the amplitude of the external stress during the network formation, but by swelling the LSCEs with a controlled amount of conventional nematic like 8CB as well. One could argue that this alters the inherent value of internal field. However, for reasons given above, the ratio g/g_c is expected to be even higher and consequently the supercriticality more pronounced in virgin LSCEs. The above methodology, based on the analysis of DNMR spectral moments, is also applicable to liquid crystals in restricted geometries, since in these systems confinement is considered phenomenologically as a source of random fields that result in a distribution of nematic order parameter values.

This work was supported by EU (HPRN-CT-2002-00169) and Slovenian Research Agency (J1-6539).

[1] M. Warner and E. M. Terentjev, *Liquid Crystal Elastomers* (Clarendon, Oxford, 2003).
[2] E. R. Zubarev, S. A. Kuptsov, T. I. Yuranova, R. V. Talroze, and H. Finkelmann, Liq. Cryst. **26**, 1531 (1999).
[3] S. Conti, A. DeSimone, and G. Dolzmann, Phys. Rev. E **66**, 061710 (2002).
[4] J. Küpfer and H. Finkelmann, Macromol. Chem. Phys. **195**, 1353 (1994).
[5] P. Martinoty, P. Stein, H. Finkelmann, H. Pleiner, and H. R. Brand, Eur. Phys. J. E **14**, 311 (2004); E. M. Terentjev and M. Warner, *ibid.* **14**, 323 (2004); O. Stenull and T. C. Lubensky, *ibid.* **14**, 333 (2004).
[6] J. Küpfer, E. Nishikawa, and H. Finkelmann, Polym. Adv. Technol. **5**, 110 (1994).
[7] S. Disch, C. Schmidt, and H. Finkelmann, Macromol. Rapid Commun. **15**, 303 (1994).
[8] J. Thoen, H. Marynissen, and W. Dael, Phys. Rev. A **26**, 2886 (1982); G. B. Kasting, C. W. Garland, and K. J. Lushington, J. Phys. (Paris) **41**, 879 (1980).
[9] M. Hébert, R. Kant, and P.-G. deGennes, J. Phys. I (France) **7**, 909 (1997).
[10] J. V. Selinger, H. G. Jeon, and B. R. Ratna, Phys. Rev. Lett. **89**, 225701 (2002).
[11] P.-G. deGennes, C.R. Acad. Sci., Ser. B **281**, 101 (1975).
[12] J. Küpfer and H. Finkelmann, Makromol. Chem. Rapid Commun. **12**, 717 (1991).
[13] P. Pasini, G. Skačej, and C. Zannoni (to be published).
[14] H. Yao, K. Ema, and C. W. Garland, Rev. Sci. Instrum. **69**, 172 (1998).